Resonant Tank Comparison of LC, LCC, and LCLC with Paralleled Inverter for Possible Surface Treatment Applications

Anumeha Kumari, Tsai-Fu Wu, Yun-Hsiang Chang, and Jui-Yang Chiu
Department of Electrical Engineering
National Tsing Hua University, Hsinchu, Taiwan
tfwu@ee.nthu.edu.tw

***Abstract*- This paper presents a resonant tank (RT) comparison of *LC*, *LCC*, and *LCLC* with paralleled inverter to generate plasma sources for possible material surface treatment. The compared multi-inverter system consists of three inverters with their outputs connected to the same load. Based on the aspects of sensitivity analysis, gain plots, simulation results and THD, the configurations of 2nd, 3rd, and 4th-order RTs are discussed. The inverters with these three types of Resonant tanks with the unified phase shift and phase-difference controls are adopted to achieve identical output currents. Simulated results of two-module inverter system have demonstrated the analyses and discussions. Hardware measurements from two-modular parallel connected inverter systems with *LCLC- D'* RT have been also presented and to further verify the theoretical analyses simulation results of three inverter connected in parallel with ± 5-10% parameter difference has been also presented in this paper.**

***Index Terms*—Resonant inverter, Parallel inverter, Resonant tanks, Sensitivity analysis, Gain-plot, Component tolerance, Phase-shift control, Phase-difference control, Unified PSM, Equal current distribution**.

I. INTRODUCTION

In modern times, high-frequency power inverters are utilized to produce plasma at atmospheric pressure [1]. This type of plasma has found widespread use in various industries, including surface treatment, medical applications, household appliances, air purifiers, and bacterial deactivation. The use of oxygen as the process gas in plasma treatment has earned it the name "oxygen plasma" [2], [3]. Typically, vacuum plasma treatment is carried out, with a gas ionized by free-moving electrons in negative and positive states [4]. The plasma chamber comprises a substrate, a target, and argon gas used for plasma generation [5]-[7].

This paper develops a power supply for possible surface treatment applications with high frequency and high output voltage. A Paralleled inverters can achieve a very high-power range, which reduces the ripple of output current, improves reliability of power system design, and increases system efficiency [8]-[9]. The major problem with paralleled structure is achieving equal power and current distribution. Since inverter systems exist parameter tolerance. In inclusion, the gate driver delays, control delay and other forms of unreliability may also consequence of output current difference.

There have been various control strategies presented to ensure that the output currents are equally distributed among inverters. The master-slave control strategy has been used when inverter modules have similar component values, whereas the phase-shift and phase-difference controls are employed when component values differ [9],[13]-[14]. This paper adopts a unified phase-shift modulation (PSM) for two parallelly connected inverters to achieve identical current and power distribution for plasma surface treatment applications [8]. Most of papers select series-parallel and series-series LCLC resonant tanks (RT) to achieve the desired outputs. This paper investigates the selection of resonant tanks from the 2nd to 4th orders.

The structure of the paper is as follows. Section II presents the resonant tank design procedures of 2nd, 3rd and all possible candidate determination of 4th order resonant tanks and includes the sensitivity analysis of the *LC*, *LCC*, *LCLC-D* and *LCLC- D'* RTs. Moving on to Section III, we detail the calculations of the overall volume, conduction loss, and circulating current, as well as the simulated output current THDs of the inverters with the RTs. The control strategy for achieving identical output current and power is described in Section IV. We present simulated results of two modules of *LCLC- D'* RTs, as well as their experimental results to verify the discussions and analyses in Section V. In this section the simulation results of three inverter with ± 5-10% component tolerance have been also presented. Finally, we offer a brief conclusion in Section VI.

II. RESONANT TANK DESIGN, GAIN PLOT AND SENSITIVITY ANALYSES OF RTs

To enable surface treatment applications, the inverter's output load is constructed with a chamber that resembles a fluorescent tube. The chamber requires an ignition followed by an inrush current to maintain ionization. Fig. 1 illustrates three possible 2nd, 3rd, and 4th order RTs that can be used.

While a 2nd order RT is generally sufficient for an inverter design. But the simple LC RT may not be suitable enough for the multiple inverters connected to the same load. To select the appropriate RT for the inverters, we have included a sensitivity analysis of the 2nd, 3rd and 4th order RTs to the component variations has been shown in subsection *C*.

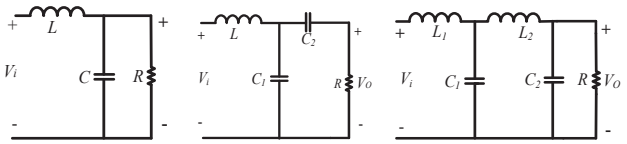

(a) *LC* (2nd order) (b) *LCC* (3rd order) (c) *LCLC* (4th order)

Fig. 1. Resonant tank structures: (a)*LC*, (b)*LCC*, and (c)*LCLC*.

Fig. 1(a) illustrates the series-parallel type of the 2nd order RT. To determine the appropriate component values for this configuration, we have considered the resonant frequency (ωr) and quality factor (Q). The values we have selected are provided below.

$$\omega_r = \omega_n \sqrt{1 - 1/Q^2} \tag{1}$$

and

$$Q = \frac{R}{\sqrt{L/C}} \tag{2}$$

Where, the Q is 4 and ω_r is lower than the operating frequency, f_s = 40 kHz, to achieve zero-voltage switching (ZVS). Thus, under ω_r = 37 kHz, the value L = 45.688 μH and C = 388.507 nF.

The LCC RT circuit configuration, illustrated in Fig. 1(b). Basically, L_1 and C_1 are supposed to filter out most of the harmonic components, since harmonic components will flow through C_2 to R which is not allowed. Thus, LCC filter functions as an *LC* filter. That is why we still use the LC resonant tank values, that is, L = 45.688 μH and $C_1 = C_2$ = 388.507 nF.

A. *Possible Candidates of the LCLC RT Determination:*

In order to provide the necessary inrush current to the output chamber, a capacitor must be connected in parallel to the load, or equivalently, in parallel. Furthermore, the inductor should add series with the transformer, so that it can help to absorb the leakage inductance of the transformer. As a result, there are four potential candidates for the 4th order resonant tanks, as illustrated in Fig. 2. We must carefully evaluate each option to determine the best fit for our system based on the required specifications.

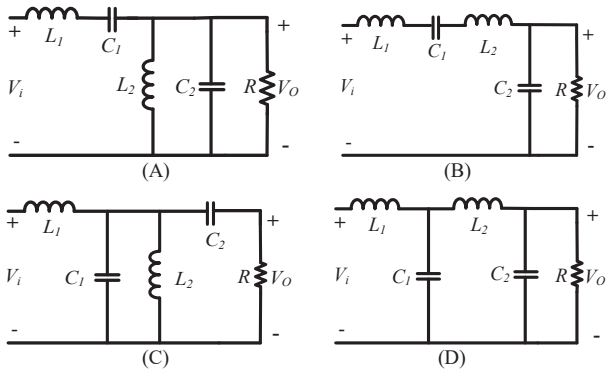

Fig. 2. Possible candidates of *LCLC* resonant tank configurations.

The circuit configurations (A) and (B) shown in Fig. 2 can block the dc component of the input voltage because of the capacitor C_1 and configuration (C) and (D) shown in Fig. 2 are connected in parallel without dc blocking capacitor. The first L_1C_1 resonant tank filters out switching frequency harmonics and the other L_2C_2 RT filters out the rest of the higher order harmonics. Based on the resonant frequency (ω_r) and the quality factor(Q) which are shown in equation can find out resonant tanks value for all 4 possible candidates of *LCLC* resonant tanks. Nature frequencies ω_n and the quality factor Q individually at the series, parallel and series- parallel branches are derived as follows:

For series connected *LC* RT,

$$\omega_n = \frac{1}{\sqrt{LC}} \tag{3}$$

$$Q = \frac{1}{R}\sqrt{\frac{L}{C}} \tag{4}$$

For Parallel connected *LC* RT,

$$\omega_n = \frac{1}{\sqrt{LC}} \tag{5}$$

$$Q = R\sqrt{\frac{C}{L}} \tag{6}$$

For series-parallel connected *LC* RT,

$$\omega_n = \frac{1}{\sqrt{LC}} \tag{7}$$

$$Q = \frac{R}{\sqrt{L/C}} \tag{8}$$

where, minimum load resistance R = 42 Ω, N=1.5 and the quality factor (Q) is chosen between 1 and 5. To ensure effective filtering of high frequency harmonics, the resonant frequency (ωr) of the first L1C1 filter is set lower than the switching frequency of 37 kHz, while the resonant frequency of the L2C2 filter is selected to be higher than the switching frequency of 120-200 kHz for all four possible candidates of LCLC RTs. This approach allows for separation of the resonant frequency of L1C1 from that of L2C2. These resonant tank values, as collected in Table 1. Although these are not the optimal values, they are effective enough to filter out the high frequency harmonics. These resonant tank values of all 4 possible candidates have been used for the simulation and shown in Fig. 3.

TABLE I.
PARAMETERS OF POSSIBLE CANDIDATES OF *LCLC*

LCLC	Inductor	Capacitor
(A)	L_1 = 722.65 µH	C_1 =25.60 nF
	L_2 = 8.35 µH	C_2 = 75.79 nF
(B)	L_1 = 554.89 µH	C_1 = 33 nF
	L_2 = 9 µH	C_2 = 22 nF
(C)	L_1 = 45.69 µH	C_1 = 388.51 nF
	L_2 = 5 µH	C_2 = 12 nF
(D)	L_1 = 45.69 µH	C_1 = 388.51 nF
	L_2 = 9 µH	C_2 = 22 nF

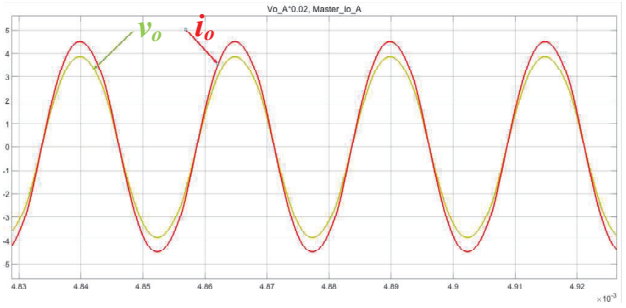

(a) *LCLC -A*

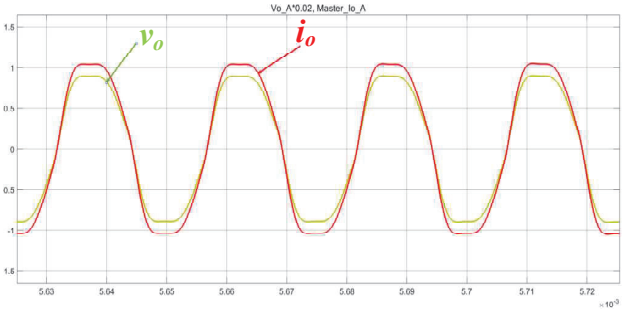

(b) *LCLC -B*

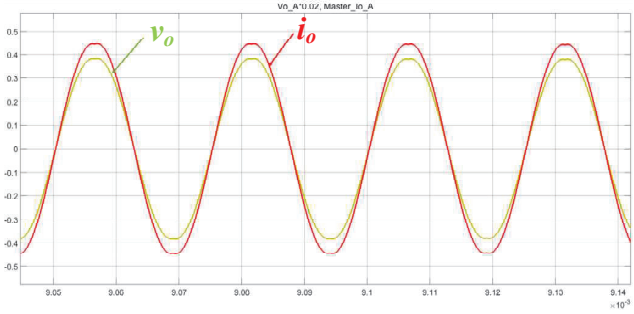

(c) *LCLC -C*

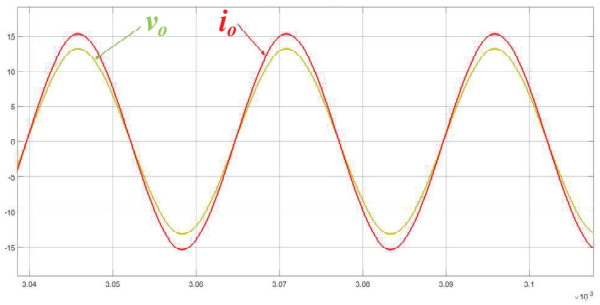

(d) *LCLC -D*

Fig. 3. Simulated results of the 4-possible candidates *LCLC* RT. (V_O: 200V/div, I_{O1}: 5A/div, V_{DC} =250 V, and R= 42 Ω)

From Fig. 3, configurations (B) and (C) are not suitable for this system, because they are not reaching the required specification output voltage and current. Thus, here two configurations (A) and (D) have been used, and we need to select one configuration with the best results for the parallel inverter system in the possible surface treatment applications. For obtaining the best configuration of the possible candidates, the next section shows the sensitivity analysis.

B. Sensitivities Plot of the LC, LCC, and LCLC Resonant Tanks:

To evaluate whether the performance of the system is susceptible to component variations, we have conducted a sensitivity analysis on the input-to-output voltage transfer function. This analysis allows us to determine the impact of component tolerance on system performance.

From Fig.4 the 2nd -order RT has the very high sensitivity with respect to L and C variations and the sensitivity of 3rd-order (*LCC*) with respect to C_2 have lowest sensitivity but with respect to L_1 and C_1 is still very high as shown in Fig. 5.

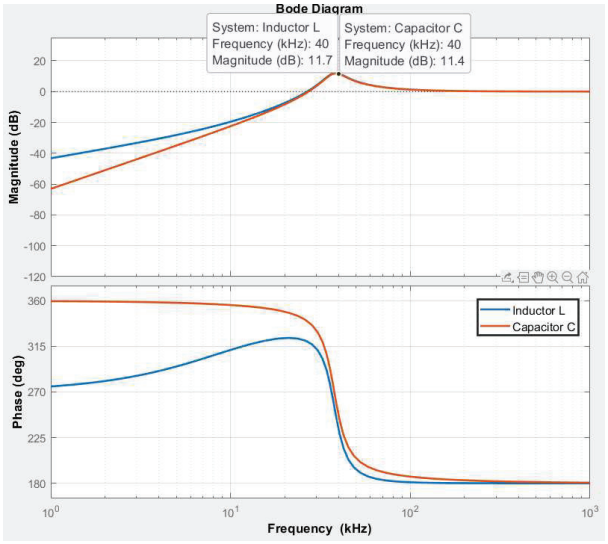

Fig. 4. Sensitivity plots of the 2nd order (LC) transfer function to L and C.

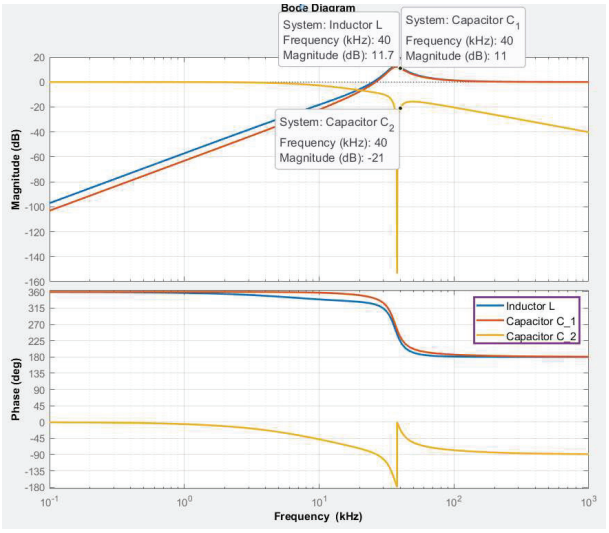

Fig. 5. *LCC* Sensitivity plots to L, C_1 and C_2.

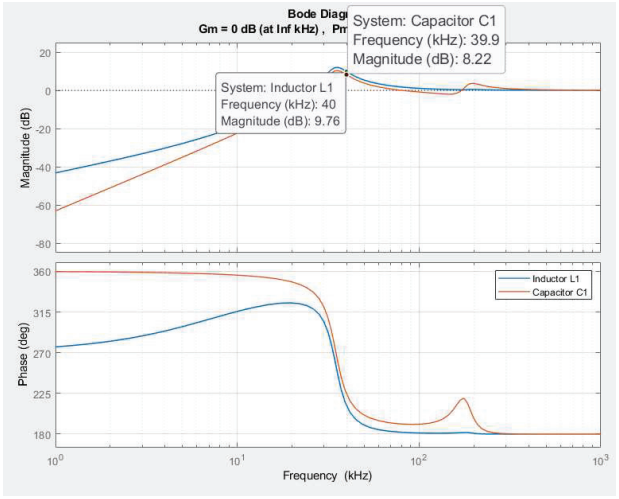

(a)

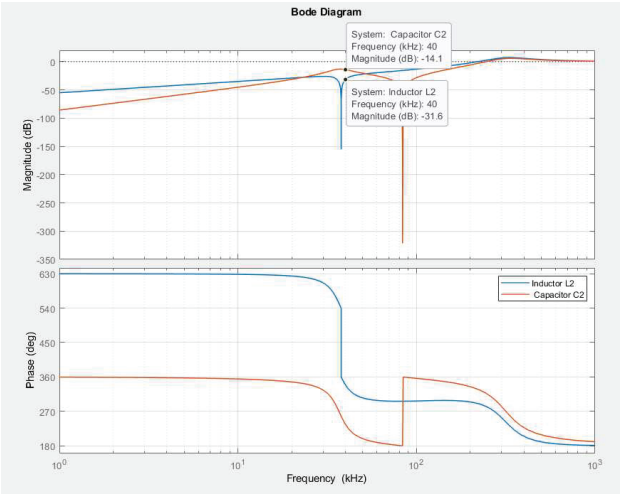

(b)

Fig. 6. *LCLC -D* Sensitivity plots to (a) L_1, C_1 and (b) L_2, C_2.

From Fig. 6(b), it can be observed that the 4th-order-D (*LCLC -D*) RT exhibits the least sensitivity concerning variations in L_2 and C_2. However, the sensitivities towards variations in L_1 and C_1 from Fig. 6(a) are relatively higher, making

it challenging to maintain identical output currents for paralleled inverters when there is a higher component tolerance. Usually, component comes with up to 10% component tolerance [8], but the 4th-order-D method is only suitable for small component tolerance due to its high sensitivity. As a result, we have developed a new parameter system for the 4th order (*LCLC-D′*) that uses the same circuit, where the frequency separation between L_1-C_1 and L_2-C_2 slowly keeps closer to each other and finds out the new 4th order resonant tank value. The parameter design for this new system is based on an error of ±5-10% for the components. To make the calculation easy, a CAD (computer-aided-design) approach with MATLAB has been used to select a new set of 4th-order- *D′* (*LCLC-D′*) RT component values, which are N=0.3 (Tx turns ratio), L_1=L_2=182.6 µH and C_1=C_2=75 nF. With these new values, the sensitivity plots to L_1, C_1 and L_2, C_2 variations are shown in Fig. 7 (a) and (b) respectively.

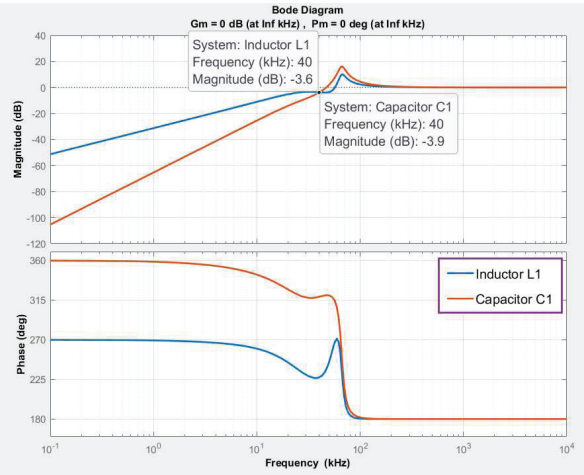

(a)

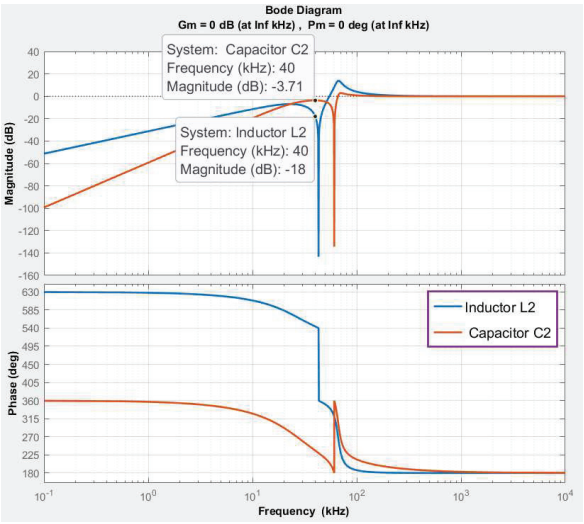

(b)

Fig. 7. *LCLC- D′* Sensitivity plots to (a) L_1, C_1 and (b) L_2, C_2.

Table II presents the sensitivities measured at the operating frequency of 40 kHz. We can observe that the 4th-order- *D′* resonant tank has the negative sensitivity to L_1, C_1 and L_2, C_2 at the operating frequency of 40 kHz. Therefore, the *LCLC- D′* RT has been used in terms of sensitivity issue for the paralleled inverter system.

TABLE II.
LIST OF SENSITIVITIES

	Sensitivities to Inductor			
Frequency	**2nd order (*LC*)**	**3rd order (*LCC*)**	**4th order-*D* (*LCLC*)**	**4th order *D′* (*LCLC*)**
	L	*L*	L_1 & L_2	L_1 & L_2
40 kHz	11.7 dB	11.7 dB	9.76 dB & -31.6 dB	**-3.6 dB & -18 dB**
	Sensitivities to Capacitor			
Frequency	**2nd order (*LC*)**	**3rd order (*LCC*)**	**4th order-*D* (*LCLC*)**	**4th order *D′* (*LCLC*)**
	C	C_1 & C_2	C_1 & C_2	C_1 & C_2
40 kHz	11.4 dB	11 dB & -21 dB	8.22 dB & -14.1 dB	**-3.9 dB & -3.71 dB**

III. CALCULATIONS OF OTHER PERFORMANCE ASPECTS

In addition to sensitivity of the inverters with various RTs, the other performance aspects are also discussed in this section. The operating frequency of the inverter is fixed to 40 kHz; and an input dc voltage of 250~ 310 V and the maximum load current of 25-30 A are considered. The switching element adopted here is SiC MOSFET for this system. The losses of switching elements in this system are divided into conduction loss and switching loss. They are calculated with MATLAB/Simulink and shown in Table III.

Conduction loss - The switching element used in this paper is the C2M0025120D produced by CREE Semiconductor Corporation. Its V_{DS} is rated 1200 V, I_{DS} is rated 90 A, $R_{DS(on)}$ is 25 mΩ and $Coss$ is 220 pF. The conduction loss is calculated from (11), where $I^2_{O,\,RMS}$ is the total rms output current of resonant tanks.

$$P_{cond} = I^2_{O,RMS} \times R_{DS(on)} \times 2 \tag{9}$$

The conduction loss of the power switch can be effectively reduced when the $R_{DS(on)}$ is smaller.

Switching loss - In the part of switching loss, since this study is within the load matching range, zero-voltage switching (ZVS) can be achieved at turn-on transition. The switching loss can be calculated from (12), where t_r and t_f are the rise and fall time, V_{in} is the input voltage of the system, I_o is the output current, and f_{sw} is the switching frequency.

$$P_{sw} = \frac{1}{2} \times V_{in} \times I_O \times (t_r + t_f) \times f_{sw} \tag{10}$$

The switching loss of resonant tanks has been shown in Table III and that of LCLC-B is less than other resonant tanks, so that it is good option for parallel inverter.

Volume – The volume depends on the core used in the system. The inductor core selected in this research for 2nd and 4th order are High Flux series CH740026 and CH610026, respectively. The 3rd order (LCC) system uses one more capacitor, so that the volume is more compared to the LC resonant tanks.

After the calculation, the volume of *LCLC-B* is less than other resonant tanks which has been shown in Table III.

Ease of Control – The phase shift and phase difference control can be easily applied to the inverter with LCLC compared to LC and LCC because there are two filtrations in LCLC resonant tank. The first L_1C_1 resonant tank filters out switching frequency harmonics and the other L_2C_2 RT filters out the rest of the higher order harmonics. With phase shift and phase difference control, they can easily achieve the desired output results.

Output current THD- As the THDs of *LC*, *LCC*, and *LCLC- D′* shown in Table III, the THD of *LCLC-* D′ is the lowest as compared to other resonant tanks.

The performance aspects including conduction loss, switching loss, volume, ease of control and output current THD of resonant tanks are collected in Table III.

TABLE III.
PERFORMANCE ASPECTS

Items		*LC*	*LCC*	*LCLC- D′*
Conduction Loss		45 W	53 W	35 W
Switching Loss		26.13W	30.W	18.54W
Volume		1174 cm^3	1225 cm^3	869 cm^3
Ease of Control		Not Easy	Not Easy	Easy
Output current THD	I_{o1}	3.49%	5.34%	0.43%
	I_{o2}	4.39%	4.74%	0.80%

IV. CONTROL STRATEGY

All of the inverter modules in the system have an identical configuration, consisting of a full-bridge topology, high frequency transformer, LCLC resonant tank, and load. The microcontroller used in this study is the 32-bit RX62T, with a maximum clock rate of 100 MHz, high-speed 12-bit, and 10-bit analog-to-digital converters (A/D converters), and multifunction timers (MTU, GPT). To monitor the system's performance, feedback signals for dc link voltage, output voltage, output current, switching current, and zero-crossing are sent to the control board. After being converted to digital signals through A/D conversion, these signals are processed through various interrupt trigger programs. These programs perform tasks such as protection, determining the phase-shift angle, and controlling working modes to ensure the safety and stability of the system.

The Symmetrical Phase-Shift Modulation (PSM) [8] technique, while effective in controlling magnitude, fails to address phase discrepancies resulting from component tolerance. This method is limited to single resonant inverters as it cannot control phase. To overcome this limitation and address current sharing issues in parallel systems, a new modulation technique known as Unified PSM has been introduced [8]. To shed light on this innovative approach, a concise discussion follows.

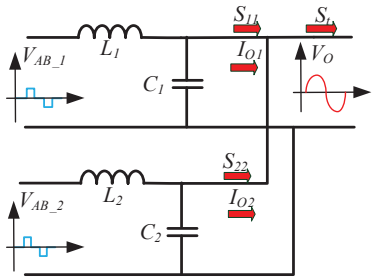

Fig. 8. Schematic diagram of an ideal LC resonant inverter.

Fig. 8 shows a schematic diagram of an ideal *LC* resonant inverter where V_{AB_1} is the voltage generated by the full bridge resonant inverter. V_{AB_1} is expanded by Fourier series, as shown in (11), where the resonant tank is assumed to be a perfect filter and the output voltage V_o is a perfect sine wave, such as (12). By multiplying (11) and (12), the average value of the multiplication of different frequencies is zero, so only the basic components are left, such as (13). Therefore, it can be seen from the time domain analysis that only the fundamental component can pass to the output, and the frequency domain analysis will be further used below. The clock frequency of the controller in this research is 96 MHz and the switching frequency is 40 kHz, so it needs to count 2,400 times.

$$V_{AB\_1} = \sum_{n=2k+1}^{\infty} \frac{4V_{dc}}{n\pi} \sin\left(\frac{D_P}{2400}\right)\pi \times \sin 2n\pi f_s t \tag{11}$$

where, $k=0,1,2..$, f_s = switching frequency, $0 \le D_P \le 1152$.

$$V_O = \sigma \sin(2n\pi f_s t + \theta_1) \tag{12}$$

$$V_{AB\_1} \times V_O = \sigma \frac{4V_{dc}}{n\pi} \sin\left(\frac{D\_point}{2400}\right)\pi \times \sin 2n\pi f_s t \times \sin(2n\pi f_s t + \theta_1) \tag{13}$$

The expressions of V_{AB_1} and V_{AB_2} in phasor forms are shown in (14) and the calculations of I_{o1} and I_{o2} are shown in (15). We multiply the output voltage ($V_O = |V_O| \angle 0°$) and current of the frequency domain to derive the real-imaginary power expansions S_{11}, S_{22}, such as (16) and (17).

$$V_{AB\_1} = |V_{AB\_1}| \angle \theta_1, \qquad V_{AB\_2} = |V_{AB\_2}| \angle \theta_2 \tag{14}$$

$$I_{o1} = \frac{V_{AB\_1} - V_O}{jX_{L1}} - \frac{V_O}{-jX_{C1}}, \quad I_{o2} = \frac{V_{AB\_2} - V_O}{jX_{L2}} - \frac{V_O}{-jX_{C2}} \tag{15}$$

$$S_{11} = V_O I^*_{O1} = \frac{|V_{AB\_1}| \times |V_O|}{X_{L1}} \angle(90° - \theta_1) - \frac{|V_O|^2}{X_{L1}} \angle 90° + \frac{|V_O|^2}{X_{C1}} \angle 90° \tag{16}$$

$$S_{22} = V_O I^*_{O2} = \frac{|V_{AB\_2}| \times |V_O|}{X_{L2}} \angle(90° - \theta_2) - \frac{|V_O|^2}{X_{L2}} \angle 90° + \frac{|V_O|^2}{X_{C2}} \angle 90° \tag{17}$$

After simplifying the (16) and (17), we can obtain (18) and (19), respectively.

$$S_{11} = V_O I^*_{O1} = \frac{|V_{AB\_1}| * |V_O|}{X_{L1}} (\sin\theta_1 + j\cos\theta_1) - j\frac{|V_O|^2}{X_{L1}} + j\frac{|V_O|^2}{X_{C1}} \tag{18}$$

$$S_{22} = V_O I^*_{O2} = \frac{|V_{AB\_2}| * |V_O|}{X_{L2}} (\sin\theta_2 + j\cos\theta_2) - j\frac{|V_O|^2}{X_{L2}} + j\frac{|V_O|^2}{X_{C2}} \tag{19}$$

As can be seen from (18) and (19), when the inductance and capacitance parameters of the two systems are identical, the

output $V_{AB\_1} = V_{AB\_2}$, and $\theta_1 = \theta_2$, the output real and the virtual power will be the same to achieve equal current sharing. But, when the parameters of the two systems are different, even with the same switching signal, the output real and virtual power will be different; that is, non-equal current sharing. Therefore, the solution is to change the switch signal to change the bold terms $|V_{AB\_1}|$, θ_1, $|V_{AB\_2}|$, θ_2 of (18) and (19), so that $S_{11} = S_{22}$, to achieve an equal current sharing.

V. SIMULATED AND EXPERIMENTAL RESULTS

This section illustrates simulated and experimental results of two parallel-connected *LCLC- D′* resonant inverters with control and without control. From simulated results, we can see that the *LCLC- D′* RT has identical output current for the paralleled inverters in case of high component tolerance.

TABLE IV.
SYSTEM SPECIFICATION

Items	Parameter
Dc input voltage	250 ~ 310 V
Output Load	42 ~ 86 Ω each 460 V ~ 650 V_{rms}
Rated power	5 Kw each
Switching Frequency	40kHz

A. *Simulated Results of the Inverter with two Parallel connected LCLC-D′ RTs:*

Fig. 9(a) and (b) show the output results of *LCLC-D′* in case of ±5% component tolerance without and with the unified phase shift modulation (PSM) control, respectively, achieving equal current distribution.

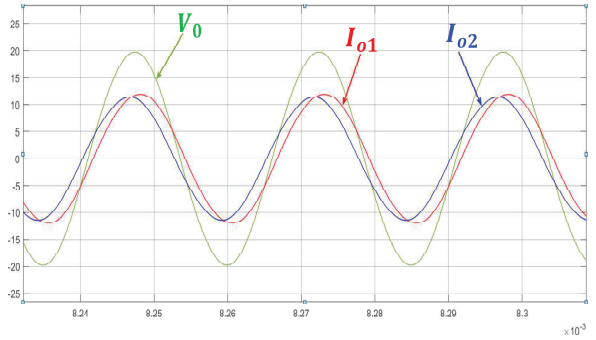

(a) (V_O: 200V/div, I_{O1}: 5A/div, I_{O2}: 5A/div)
V_{DC} =250 V, and R= 42 Ω

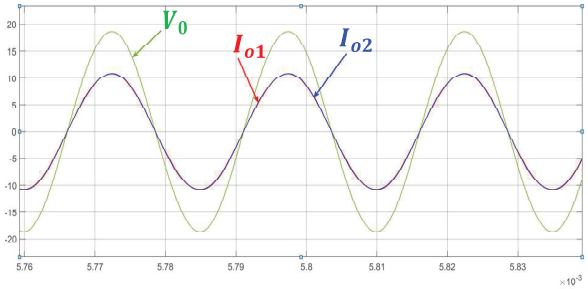

(b) (V_O: 200V/div, I_{O1}: 5A/div, I_{O2}: 5A/div)
V_{DC} =250 V, and R= 42 Ω

Fig. 9. Simulated results of two *LCLC-D′* parallel resonant inverters: (a) without and (b) with the controls. **(± 5 % tolerance)**

B. *Experimental Results of two Parallel connected LCLC-D′ Inverter:*

The inverters with different $L_1C_1L_2C_2$ filters are shown in Table IV. Fig. 10(a) shows the measured two output currents, I_{o1} and I_{o2}, of the inverters with very slightly different even without the control, while Fig. 10(b) shows those with the unified phase-shift modulation (PSM) controls. It can be observed that the output currents with the controls come out identical magnitude and phase. The real component value has been illustrated in table IV.

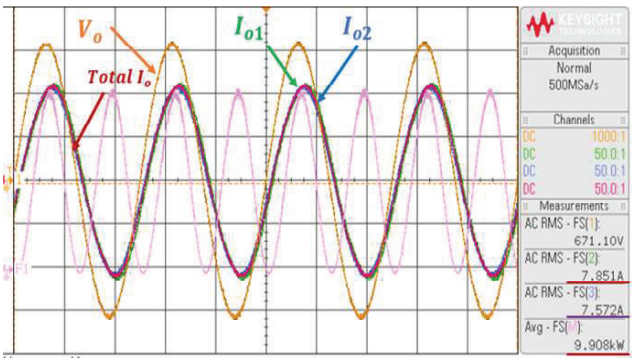

(a) (I_{O1}: 5A/div, I_{O2}: 5A/div, I_O: 10A/div, V_O: 200V/div, time: 10µs/div)

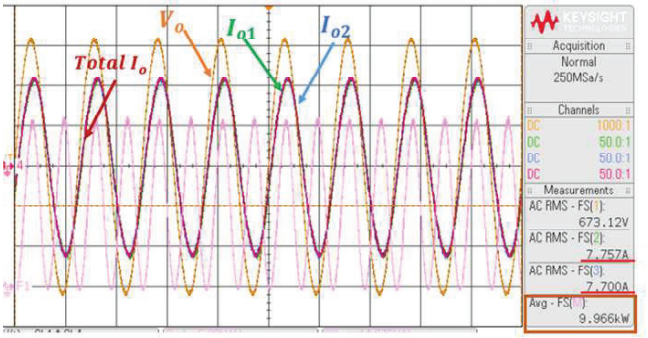

(b) (I_{O1}: 5A/div, I_{O2}: 5A/div, I_O: 10A/div, V_O: 200V/div, time: 20µs/div)

Fig. 10. Measured voltage and current waveforms at **10 kW** (a) without, and (b) with the controls.

C. *Simulated Results of Three LCLC-D′ RTs:*

To further investigate the current-sharing performance of the proposed unified phase shift control strategy, we have employed third *LCLC-D′* inverter modules with ±5% component tolerance parallelly connected to other inverters. The simulated results are depicted in Fig. 11. With the controls, their output current waveforms are almost identical, as shown in Fig. 11(b), even under 10% component variation in the third inverter, as reported in Table V. This result confirms that the unified PSM controls enable the LCLC inverters to produce output currents with nearly identical phase and magnitude, despite parameter variations. Moving forward, we plan to experiment with a 15-kW prototype of three paralleled LCLC inverters in future.

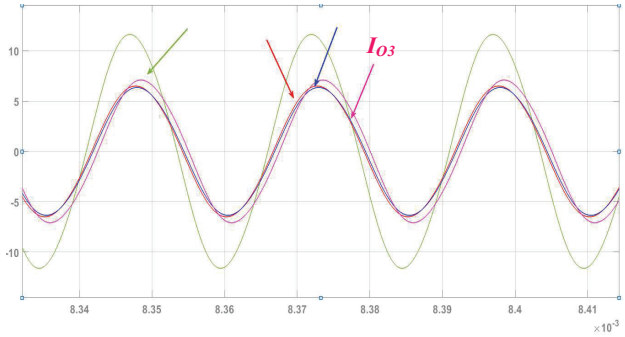

(a) (V_O: 200V/div, I_{O1}: 5A/div, I_{O2}: 5A/div)

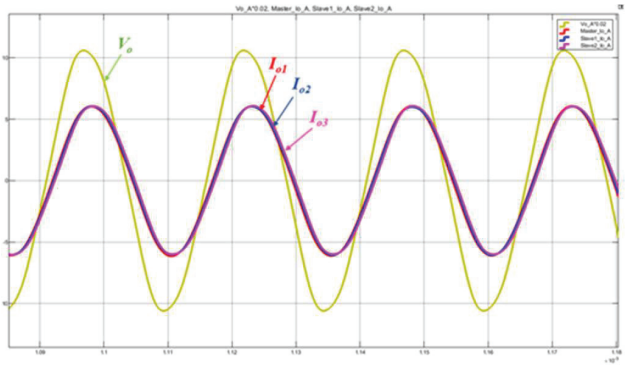

(b) (V_O: 200V/div, I_{O1}: 5A/div, I_{O2}: 5A/div)

Fig. 11. Simulated results of three *LCLC -D′* parallel resonant inverters: (V_{DC} =250 V, and R= 28Ω), (a) without and (b) with the controls.

TABLE V.
COMPONENT VALUE DIFFERENCE OF THE THREE INVETER (*LCLC- D′*)

	Inverter 1	**Inverter 2**	**Inverter 3**
Inductors L_1=L_2	182.659 μH	184.676 μH	165.516 μH
Capacitors C_1=C_2	75.162 nF	74.232 nF	77.449 nF

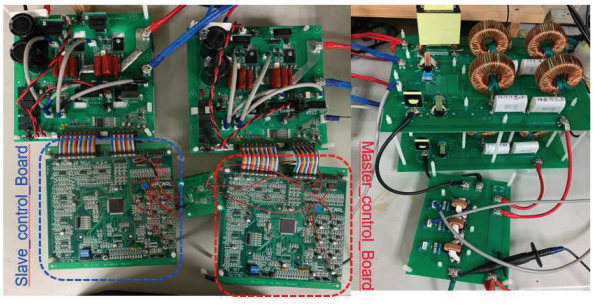

Fig. 12. Image of Two Paralleled Inverters with LCLC-D′ RTs Prototype.

VI. CONCLUSION

This paper presents an in-depth analysis and discussion of three paralleled inverters with LCLC RTs, which were designed and implemented to generate plasma sources for material-surface treatment. The inverters, each with a power rating of 5 kW, were connected in parallel with *LCLC* RTs. Through sensitivity analyses of the 2nd, 3rd, 4th order-D, and 4th order-D′ resonant tanks, it was found that the 4th order- D′ resonant tank demonstrated the least sensitivity to component variation at the operating frequency of 40 kHz, making it well-suited for paralleled inverters. With the unified phase-shift modulation controls, the output power can be regulated to the desired value of 10 kW within the load range. Moreover, their output currents can be controlled to have identical magnitude and phase, even under component parameter variations. The simulated and measured results have validated the analyses and discussions of the designed paralleled inverters.

REFERENCES

[1] C. Huang, C. Tsai, W. Ma and K. Lai, "Optical and Glow Diagnostics of 13.56-MHz RF Plasma-PVDF Membrane Surface Interactions," in *IEEE Transactions on Plasma Science*, vol. 42, no. 10, pp. 2568-2569, 2014.

[2] C. Gong, X. Tian, S. Yang, R. K. Y. Fu and P. K. Chu, "Surface Treatment of Polyethylene Terephthalate Using Plasma Ion Implantation Based on Direct Coupling of RF and High-Voltage Pulse," in *IEEE Transactions on Plasma Science*, vol. 40, no. 2, pp. 487-491, Feb. 2012.

[3] D. Kovacik, P. Stahel, J. Rahel, and M. Cernak, "High-Speed Low-Cost Surface Treatments Using A Novel Atmospheric-Pressure Plasma Source," in *IEEE International Conference on Plasma Sciences (ICOPS)*, Antalya, pp. 1-1.

[4] P. K. Jain, G. Edwards, C. Hubbard, and D. Bannard, High Frequency Power Distribution System, US Patent No.5,444,608, 1995.

[5] Xiao-jing, Q. Guan-jun and C. Jie-rong, "The Effect of Surface Modification by Nitrogen Plasma on Photocatalytic Degradation of Polyvinyl Chloride Films," *Applied Surface Science*, Vol.254No.20, pp.6568-6574, 2008.

[6] T. Akitsu, H. Ohkawaa, M. Tsujib, H. Kimurab, and M. Kogomac, "Plasma Sterilization Using Glow Discharge at Atmospheric Pressure," *Surface and Coatings Technology*, vol.193, no.1-3, pp.29-34, 2005.

[7] R. S. Tipa and G. M. W. Kroesen, "Plasma-Stimulated Wound Healing," in IEEE Transactions on Plasma Science, vol. 39, no. 11, pp. 2978-2979, Nov. 2011.

[8] J. Liu, K. W. E. Cheng and J. Zeng, "A Unified Phase-Shift Modulation for Optimized Synchronization of Parallel Resonant Inverters in High Frequency Power System," in *IEEE Transactions on Industrial Electronics*, vol. 61, no. 7, pp. 3232-3247, July 2014

[9] M. Forouzesh and Y.-F. Liu, "Interleaved LCLC Resonant Converter with Precise Current Balancing over a Wide Voltage Range." In *IEEE Trans. Power Electronics*, vol. 36, no. 9, Sept., 2021.

[10] Z. M. Ye, P. K. Jain and P. C. Sen, "A New Control Scheme for Circulating Current Minimization in High Frequency AC Power Distribution Architecture with Multiple Inverter Modules Operated in Parallel," *31st Annual Conference of IEEE Industrial Electronics Society, 2005. IECON 2005.*, Raleigh, NC, 2005.

[11] Y. Panov, J. Rajagopalan and F. C. Lee, "Analysis and Design of N Paralleled DC-DC Converters with Master-Slave Current-Sharing Control," *Proceedings of APEC 97 - Applied Power Electronics Conference*, Atlanta, GA, USA, 1997, pp. 436-442.

[12] Tsai-Fu Wu, Yu-Kai Chen and Yong-Heh Huang, "3C strategy for inverters in parallel operation achieving an equal current distribution," in *IEEE Transactions on Industrial Electronics*, vol. 47, no. 2, pp. 273-281, April 2000.

[13] C. Takami, T. Mishima and M. Nakaoka, "A new ZVS phase shift-controlled class D full-bridge high-frequency resonant inverter for induction heating," *2012 15th International Conference on Electrical Machines and Systems (ICEMS)*, Sapporo, 2012, pp. 1-6.

[14] T.-F. Wu, Y.-E. Wu, H.-M. Hsieh and Y.-K. Chen, "Current Weighting Distribution Control Strategy for Multi-Inverter Systems to Achieve Current Sharing," in *IEEE Transactions on Power Electronics*, vol. 22, no. 1, pp. 160-168, Jan. 2007.

[15] Y. Zhongming, J. Praveen and S. Paresh, "Multiple Resonant Inverters in Parallel with a Novel Current Sharing Control Based on Current Decomposition Method," *2006 37th IEEE Power Electronics Specialists Conference*, 2006, pp.1-7.